

A direct analytical formula for calculating the fields from surface-electrodes has allowed us to use numerical optimization techniques to help in the design of surface-electrode ion traps.

Surface-electrode ion traps

Ion trapping in micro-fabricated surface-electrode traps [1] has recently been demonstrated [2]. The observed heating rates appear to be compatible with quantum information processing (QIP) [3].

Compared to traditional (3D) ion traps, surface-electrode traps have significant advantages with respect to scaling:

- Compatibility with micro-fabrication.
 - Integration with control electronics [4].
- Operational characteristics are not as good:
- Low trap depth.
 - Reduction of trapping frequency by a factor of ~ 3 for same ion-electrode distance.

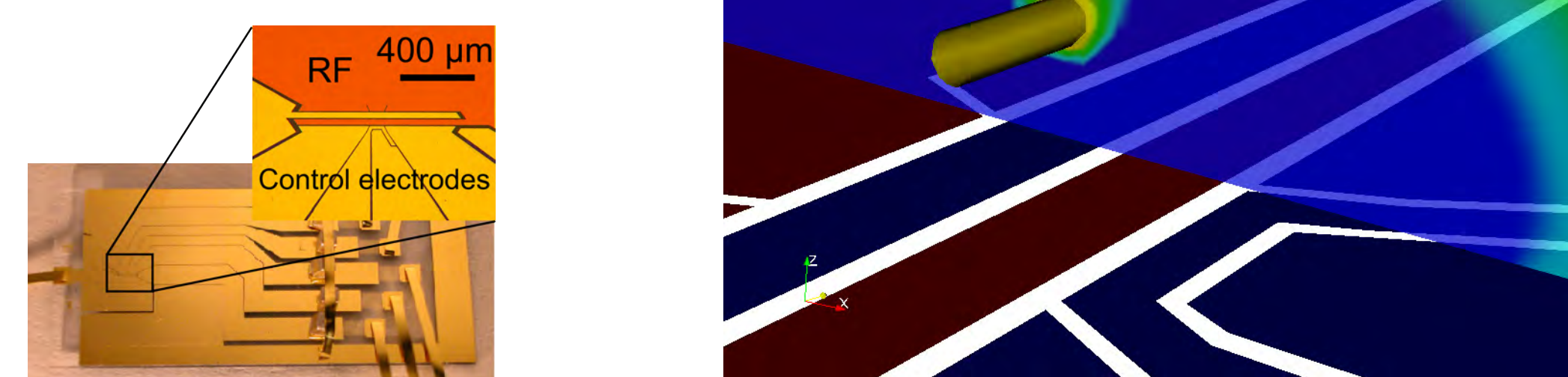
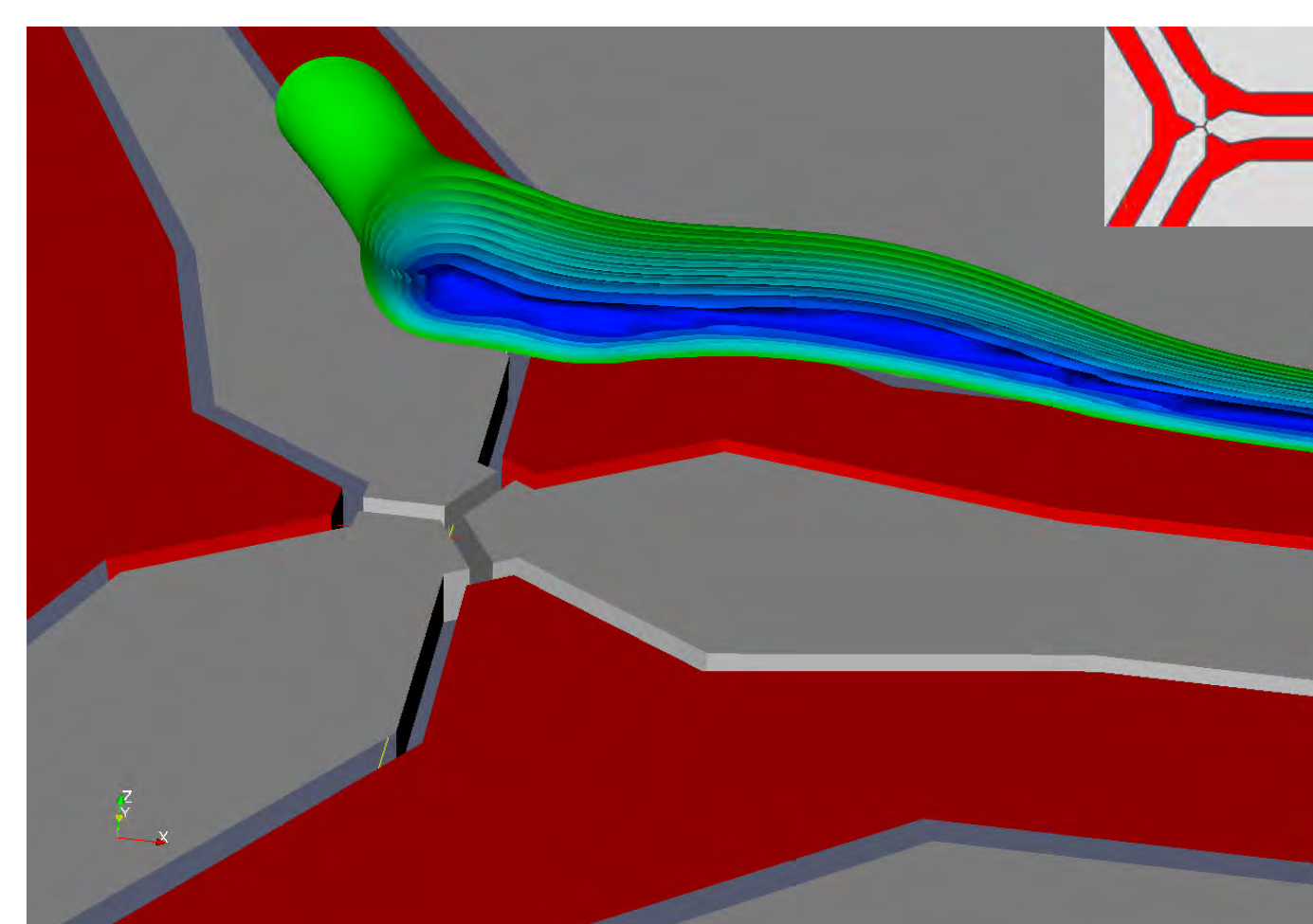


Figure 1: A single-zone surface-electrode trap recently demonstrated at NIST [2]. Leftmost part shows a picture of the trap assembly. Inset is a zoom on the trapping region with the RF electrode shaded red. Rightmost part shows the simulated ponderomotive potential, Φ_P , together with the trap electrodes. RF electrode is red, while ground and control electrodes are blue. The transparent cut-plane shows Φ_P in a plane perpendicular to the quadrupole axis. The trapping minima is located $40 \mu\text{m}$ above the surface, and the depth is approximately 200 meV for potentials in [3]. The tube is a part of the 100 meV iso-surface of Φ_P . Recent measurements of the heating rate show that the heating for Mg-ions is on the order of 0.3 quanta/ms at 5.2 MHz axial trap frequency [3].

Towards bump-free intersections

By modifying the RF electrode shapes, it is possible to reduce the the residual RF-field on the path through an intersection [5].



Current design efforts are based on

- Numerical optimization, making use of an analytical formula, Eq. (1) (see panel at right).
- Manual tweaking to satisfy production constraints and counter the effects of electrode separation.

Residual RF field

As illustrated by Fig. 3, even the optimized electrodes have a residual RF field on the path through the intersection.

- The maximal Φ_P is reduced by two orders of magnitude.
- The maximal curvature of Φ_P is virtually unchanged.

The residual curvature appears to be prohibitive to fully controlled ion transport.

Figure 2: An example of a ponderomotive potential with reduced bumps obtained by modifying electrode shapes. This intersection has the same boundary conditions as that of Fig. 4. This form of the intersection is used in the multi-zone surface electrode trap currently being built at NIST [6]. The figure elements are the same as those of Fig. 4.

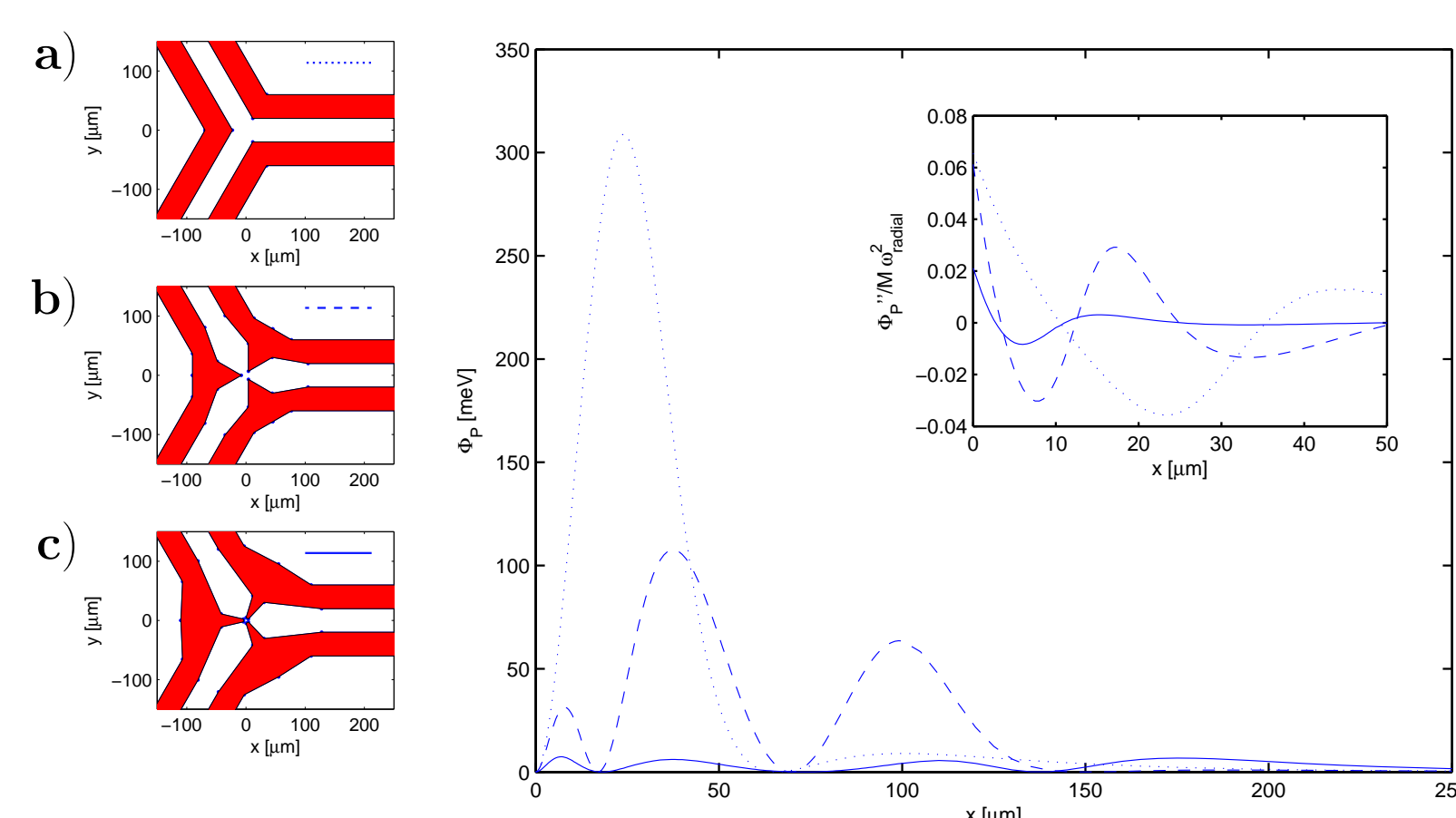


Figure 3: The residual Φ_P on the path through three y-intersection designs, calculated according to Eq. (1). The maximal value of Φ_P for design **c** is reduced by two orders of magnitude compared to that of the naive design, **a**. The inset shows the curvature of Φ_P along the path, relative to the asymptotic transverse curvature of Φ_P in the arms of the intersection. This value is only slightly reduced for the optimized geometries.

Trap networks

Ion-trap networks have been suggested as large-scale QIP systems [7]. Intersections between trapping regions are a key ingredient of such trap networks.

As illustrated by Fig. 4, the naive implementation of an intersection for a surface-electrode trap is troubled by the lack of path of constant Φ_P through the intersection. This is critical for several reasons:

- The residual RF-field may cause motional heating.
- Controlled transport of multi-species ion groups through the intersection is complicated.
- A high gradient or curvature of Φ_P makes it difficult to transport ions in a controlled fashion using variable control potentials.

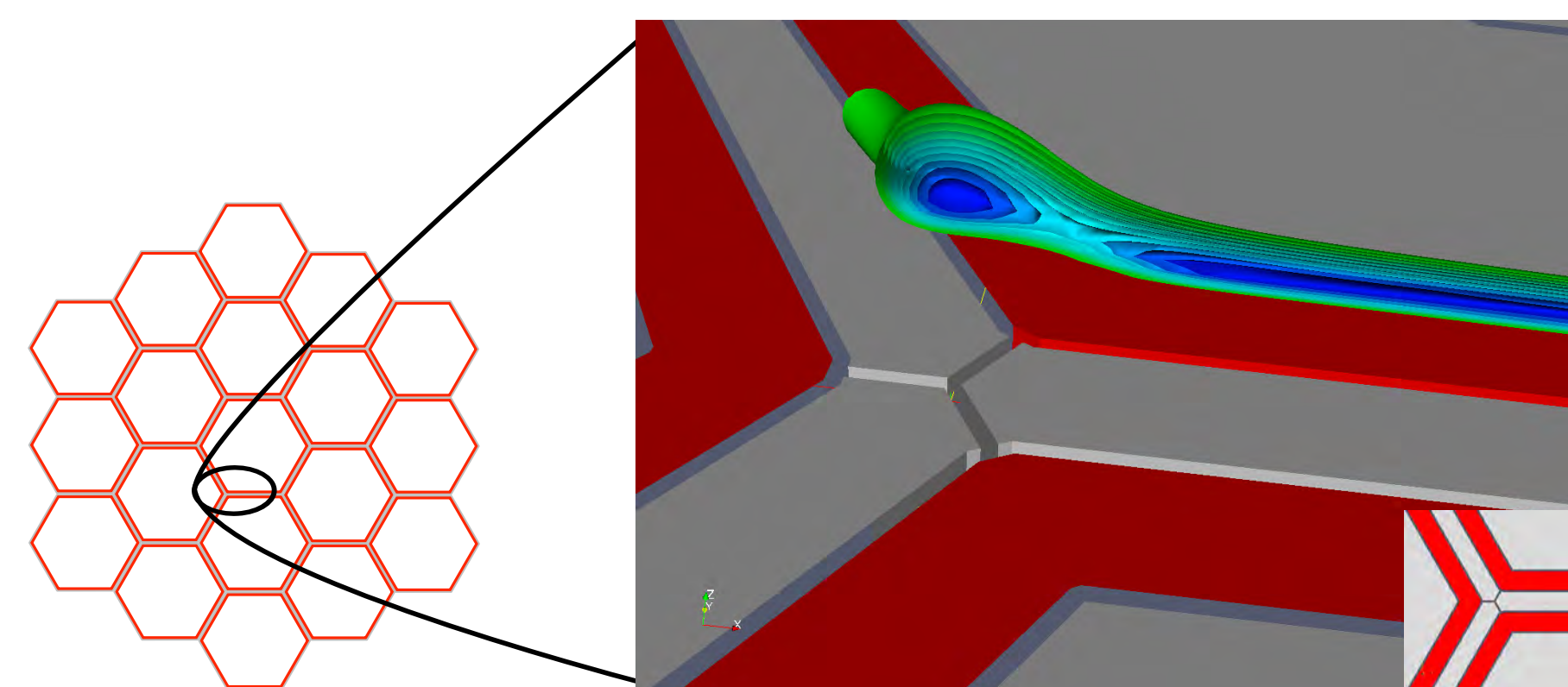


Figure 4: A naive implementation of a y-junction for a surface-electrode trap network. Red areas on the surface indicate RF electrodes, gray areas are RF ground (either ground or control electrodes). Iso-surfaces of Φ_P are shown at $100\text{-}1000 \text{ meV}$ with 100 meV spacing.

Modeling surface electrodes

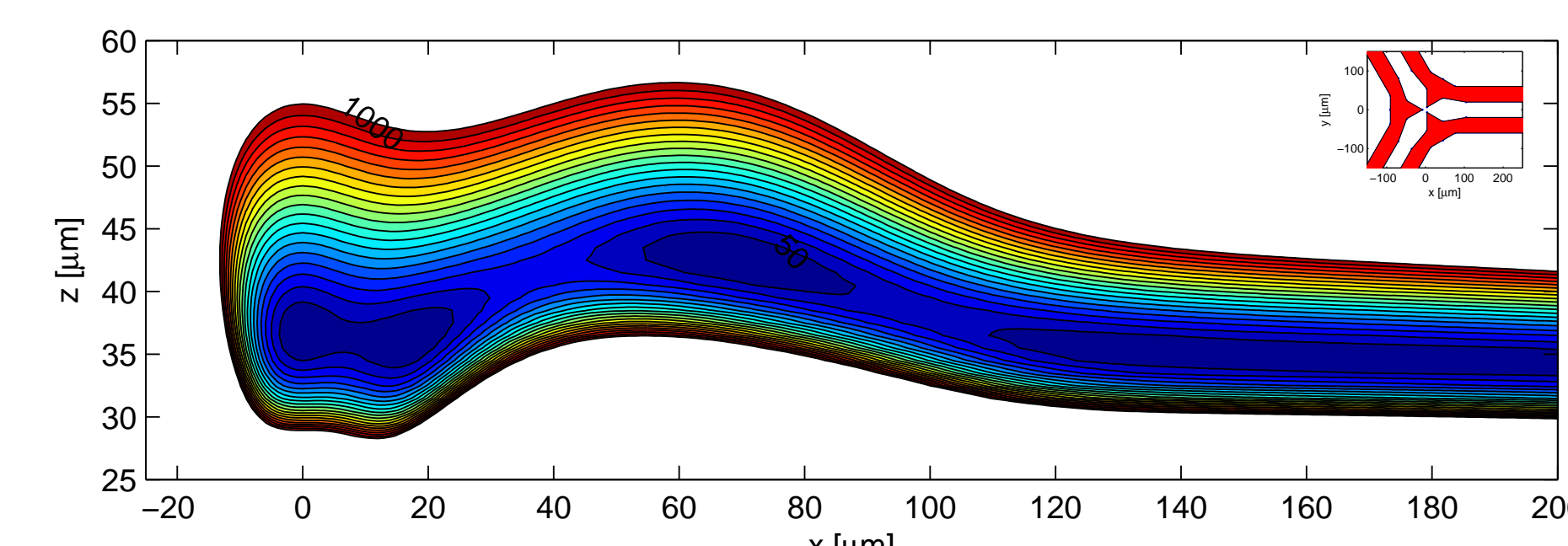
A simple analytical method [8] allows us to calculate the field from a surface electrode directly.

For a flat electrode with boundary γ embedded in an infinite grounded plane

$$\mathbf{E}(\mathbf{x}) = \frac{V}{2\pi} \oint_{\gamma} \frac{(\mathbf{x} - \mathbf{x}') \times ds'}{|\mathbf{x} - \mathbf{x}'|^3}. \quad (1)$$

This formula does not describe (insulating) gaps between electrodes. As illustrated by Fig. 5, this does not appear to strongly influence the ponderomotive potential.

Analytical



Numerical

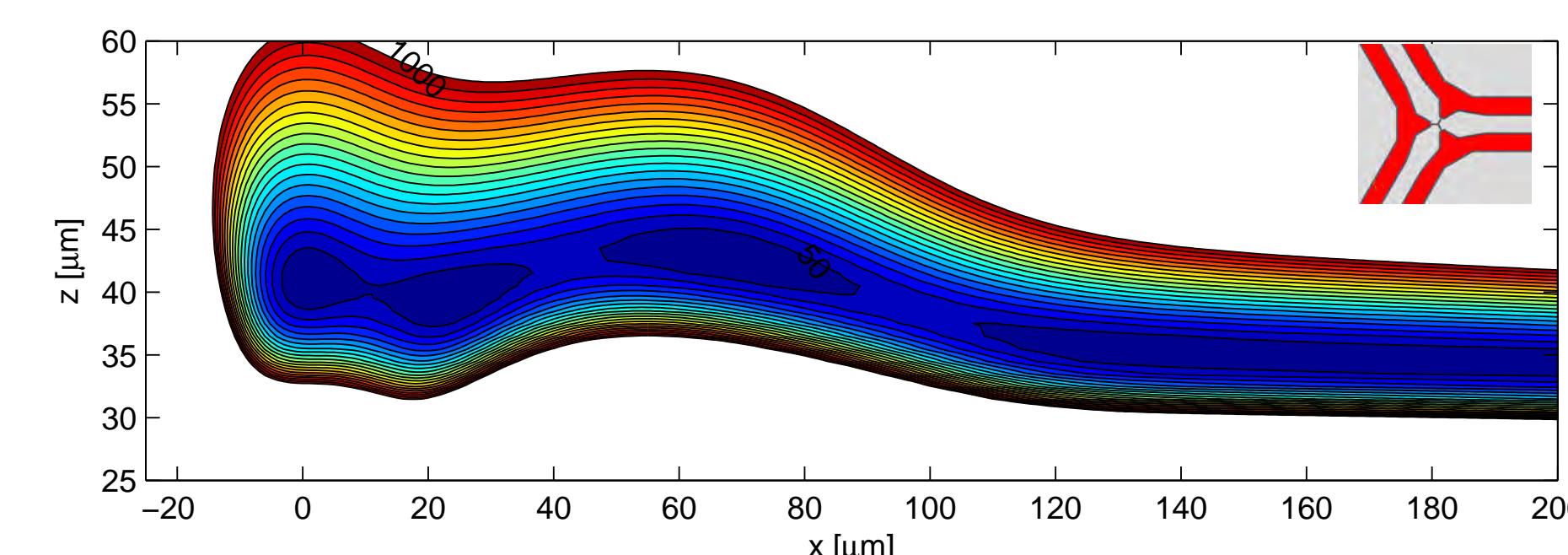
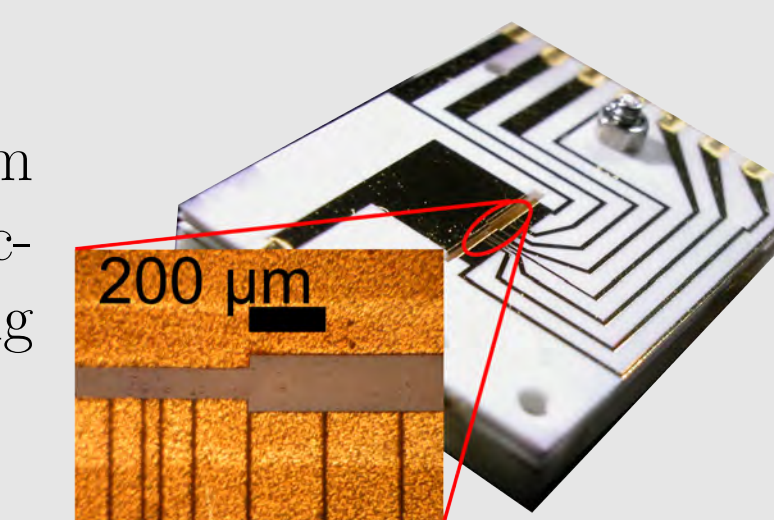


Figure 5: Comparing Φ_P obtained by Eq. (1) and boundary element method (BEM) simulations, the latter including realistic gaps between electrodes. Contour plots show the value of Φ_P in meV on the x - z plane. Rightmost plots show the position of the Φ_P minimum as a function of x and the value of Φ_P at the minimum. Analytical results are for design **b** of Fig. 3. Numerical results are for the geometry described in Fig. 2.

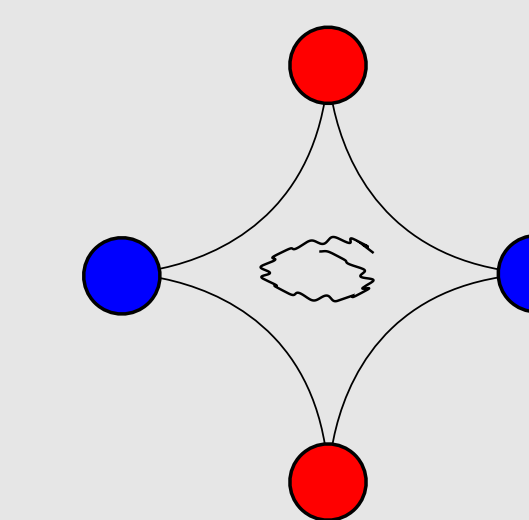
RF ion traps

RF electrodes (Red). Provide a radio frequency oscillating (quadrupole) field, establishing a ponderomotive potential, Φ_P .
Control electrodes. Serve as RF ground, and provide an adjustable potential superimposed on the ponderomotive potential.

The 3D traps currently used for QIP at NIST are made from gold-plated laser-machined alumina. Segmented control electrodes allow the ions to be moved between different trapping zones along the symmetry axis.



Ponderomotive potential



In the limit of large RF frequency, Ω_{RF} , the effect of the RF field can be described by a ponderomotive potential equal to the average kinetic energy due to the micro-motion:

$$\Phi_P = \langle E_{\text{kin,mm}} \rangle = \frac{|\mathbf{E}_{\text{RF}}^{(0)}|^2}{4M\Omega_{\text{RF}}^2}$$

The RF field result in a fast oscillatory *micro-motion* being superimposed on the slower *secular motion* of the ion, as illustrated by the jittery trajectory.

When Φ_P is given in units of energy on this poster, we assume the RF drive voltage to be 1 V , $M = 1 \text{ amu}$, and $\Omega_{\text{RF}} = 2\pi \cdot 1 \text{ MHz}$.

Ideal intersections

The laws of electrodynamics do allow potentials corresponding to intersections. Whether or not such potentials can be produced by surface-electrodes is still under investigation.

RF potential amplitudes:

$$\begin{aligned} \phi_a &= xyz \\ \phi_b &= y(y^2 - 3x^2)z \\ \phi_c &= z^4 - 3(x^2 + y^2)z^2 + 3x^2y^2 \\ \phi_d &= -8z^6 + 60(x^2 + y^2)z^4 \\ &\quad - 45(x^2 + y^2)^2z^2 \\ &\quad + 5(y^3 - 3x^2y)^2 \end{aligned}$$

Iso-surfaces for the ponderomotive potentials corresponding to the RF potential amplitudes ϕ_i listed on the right. The ponderomotive potential has field-free lines emerging along 4 (**a, c**) and 6 (**b, d**) directions in the x - y plane.

References

- [1] J. Chiaverini et al., Quantum Information and Computation **5**, 419 (2005).
- [2] S. Seidelin, J. Chiaverini, et al., Phys. Rev. Lett. **96**, 253003 (2006).
- [3] R. J. Epstein et al., Poster at this conference (2007).
- [4] J. Kim et al., Quantum Inf. Comput. **5**, 515 (2005).
- [5] R. Reichle et al., Poster at NIST Workshop on Trapped Ion Quantum Computing (2006), URL <http://tf.nist.gov/ion/workshop2006/t01.pdf>.
- [6] J. Amini et al., Poster at this conference. (2007).
- [7] D. Kielpinski, C. Monroe, and D. J. Wineland, Nature **417**, 709 (2002).
- [8] M. H. Oliveira and J. A. Miranda, Eur. Jour. Phys. **22**, 31 (2001), physics/0011015.